Geomorphology 138 (2012) 121–129

Contents lists available at SciVerse ScienceDirect

Geomorphology

journal homepage: www.elsevier.com/locate/geomorph

Southern Appalachian hillslope erosion rates measured by soil and detrital radiocarbon in hollows

T.C. Hales [a,*], K.M. Scharer [b], R.M. Wooten [c]

[a] Earth Surface Processes Research Group, School of Earth and Ocean Sciences, Cardiff University, Cardiff, UK
[b] Department of Geology, Appalachian State University, Boone, NC, USA
[c] North Carolina Geological Survey, Swannanoa, NC, USA

ARTICLE INFO

Article history:
Received 14 December 2010
Received in revised form 29 August 2011
Accepted 31 August 2011
Available online 8 September 2011

Keywords:
Appalachians
Hillslope processes
Radiocarbon analysis
Creep erosion
North Carolina

ABSTRACT

Understanding the dynamics of sediment generation and transport on hillslopes provides important constraints on the rate of sediment output from orogenic systems. Hillslope sediment fluxes are recorded by organic material found in the deposits infilling unchanneled convergent topographic features called hollows. This study describes the first hollow infilling rates measured in the southern Appalachian Mountains. Infilling rates (and bedrock erosion rates) were calculated from the vertical distribution of radiocarbon ages at two sites in the Coweeta drainage basin, western North Carolina. At each site we dated paired charcoal and silt soil organic matter samples from five different horizons. Paired radiocarbon samples were used to bracket the age of the soil material in order to capture the range of complex soil forming processes and deposition within the hollows. These dates constrain hillslope erosion rates of between 0.051 and 0.111 mm yr^{-1}. These rates are up to 4 times higher than spatially-averaged rates for the Southern Appalachian Mountains making creep processes one of the most efficient erosional mechanisms in this mountain range. Our hillslope erosion rates are consistent with those of forested mountain ranges in the western United States, suggesting that the mechanisms (dominantly tree throw) driving creep erosion in both the western United States and the Southern Appalachian Mountains are equally effective.

© 2011 Elsevier B.V. All rights reserved.

1. Introduction

Most of the sediment exiting soil-mantled orogens are derived from hillslopes. Hillslope processes are diverse and measurements of the rates of key processes, including hillslope creep, are still relatively rare (Reneau et al., 1989; McKean et al., 1993; Heimsath et al., 2001; Roering et al., 2002). Unchanneled, zero-order valleys or hollows (Hack and Goodlet, 1960) provide a record of hillslope erosion within the stratigraphy of soil deposited in their axis. Soil eroded from divergent noses and planar side slopes accumulates in hollows, where it accumulates until removed by shallow landsliding (Dietrich and Dunne, 1978). Radiocarbon dates from organic material preserved within the hollow stratigraphy can be used to estimate the hillslope sediment flux between landslide events (Reneau et al., 1986, 1989; Reneau and Dietrich, 1990, 1991). As landslides recur at millennial timescales, hollows provide estimates of hillslope creep across the Holocene (Reneau and Dietrich, 1990; Eaton et al., 2003a).

Convergent hollow topography concentrates shallow groundwater flow that periodically evacuates accumulated soil material by shallow landsliding (Dietrich and Dunne, 1978). After an initial period of rapid slope adjustment that adds material to the base of the hollow, emptied hollows progressively fill with colluvial material derived from hillslopes immediately adjacent to the hollow (Reneau et al., 1989). The initially rapid local slope response adds soil and carbon to the base of the hollow. When dated, this material can provide an estimate of the age of the landslide event. After this initial infilling (that can deposit a maximum of tens of centimetres of soil in the hollow) the hollow then accumulates eroded hillslope material (Reneau and Dietrich, 1990). For short hillslopes, soil creep is the primary erosional mechanism recorded within hollow deposits. Creep can be driven by a suite of climatically dependent processes, such as biogenic activity (Roering et al., 2002; Gabet et al., 2003; Yoo et al., 2005), wetting and drying cycles (Carson and Kirkby, 1972), or freeze–thaw (Matsuoka, 1998). The individual events controlling creep are stochastic (e.g. tree throw events typically occur at a decadal-centennial scale), making them difficult to measure at short timescales (Schumm, 1967). Methods that average across multiple sediment transport events particularly those that utilise in situ and meteoric cosmogenic radionuclides (McKean et al., 1993; Heimsath et al., 2001) and radiocarbon (Reneau and Dietrich, 1991) provide an integrated estimate of hillslope creep.

We have calculated creep erosion rates in the southern Appalachian Mountains, North Carolina by measuring hollow deposition rates. The Appalachian Mountains are a tectonically quiescent, 2600 km long mountain range that crosses a large latitudinal and climatic gradient.

* Corresponding author. Tel.: +44 2920874329; fax: +44 2920874326.
E-mail address: halest@cardiff.ac.uk (T.C. Hales).

0169-555X/$ – see front matter © 2011 Elsevier B.V. All rights reserved.
doi:10.1016/j.geomorph.2011.08.030

The effect of the climatic gradient was most pronounced during the last glacial maximum (LGM), when the northern Appalachians were extensively glaciated while the southern Appalachians were a mixture of periglacial uplands and boreal-temperate evergreen forests. Active periglacial conditions created solifluction deposits, felsenmeer, scree slopes at high elevations (Delcourt et al., 1982; Clark and Ciolkosz, 1988; Braun, 1989; Eaton et al., 2003a; Taylor and Kite, 2006; Nelson et al., 2007). Large debris accumulations in topographic hollows have been described within the geomorphic literature, mostly in the central and northern Appalachians (Mills, 1982, 1983; Mills and Allison, 1995) and are commonly thought to represent relict periglacial sedimentation (Hack et al., 1960; Eaton et al., 2003a). The only significant periglacial blockfield in the Southern Appalachian Mountains is found at >1500 m elevation in the Great Smoky Mountains (Nelson et al., 2007), suggesting that periglacial erosion may have been of restricted extent in these mountains. Today, the whole range is soil-mantled and the climatic gradient controls the ecological makeup of forests. Southern Appalachian forests have transitioned through three main assemblages since the LGM: boreal forests on upper slopes during the LGM, northern hardwood forests (dominated by sugar maple and oaks) at the highest elevations today, and cove hardwoods (dominated by chestnut, hemlock, and tulip poplar) in lower elevations today (Delcourt et al., 1982).

The soil mantle that formed during the Holocene promotes hillslope creep and shallow landsliding within the Southern Appalachian Mountains (Fig. 1; Clark, 1987; Wieczorek et al., 2004; Witt, 2005; Wooten et al., 2007). Extensive inventories of shallow landsliding, particularly within North Carolina, provide an estimate of short term landsliding rates (Fig. 1; Clark, 1987; Witt, 2005; Wooten et al., 2006, 2008, 2009); however, due to the stochastic nature of the large storms that trigger most landslides, erosion rate estimates based on these figures are strongly biassed by extreme events. Other forms of hillslope erosion, particularly creep, represent an important and as yet unquantified component of Appalachian erosion. This study attempts to understand the role that late Pleistocene to modern hillslope erosion plays in the development of Southern Appalachian hillslopes. We measured the rate of hillslope sediment deposition into hollows using detrital and soil radiocarbon based on the method pioneered by Reneau et al. (1989). This method is ideally suited to estimating erosion rates in the southern Appalachians because highly productive hardwood forests provide large reserves of soil carbon and relatively frequent fires produce large amounts of detrital carbon (Field et al., 1998; Fesenmeyer and Christensen, 2010).

2. Methods

2.1. Field location and sampling methods

We estimated hillslope erosion rates for two hollows within the Coweeta Hydrologic Laboratory, North Carolina, U.S.A. The Coweeta basin is located on the steeper, eastern side of an asymmetrical escarpment (locally called the Nantahala Mountains Escarpment; Wooten et al., 2008) with considerable relief (~900 m over the 5 km length of the basin) and a strong orographic precipitation gradient (a mean annual precipitation range of 1800 to 2300 mm; Swift et al., 1988). The basin topography is characterised by the nose and hollow topography typical of Appalachian uplands (Hack et al., 1960). The Coweeta basin has a considerable number of hollows that have failed catastrophically in the past (Hursh, 1941), most recently during the destructive Hurricanes Frances and Ivan (Fig. 1; Wooten et al., 2007, 2008). We sampled hollows within the steep upper section of the catchment, at the transition between cove hardwood and northern hardwood forest associations within one of the most productive parts of the Coweeta forest (Hwang et al., 2009).

We dated soil and charcoal from two locations in the upper part of the catchment that were excavated as part of a previous study of landslide susceptibility; Pit 13 at 1204 m and Hollow Trench at 1375 m (Hales et al., 2009) (Fig. 2). Both hollows were identified in the field as areas of convergent topography in unchanneled valleys. The Hollow Trench (Fig. 2A) is located in Coweeta Watershed 28, ~200 m below the main escarpment ridge, in a broad hollow (maximum width of 70 m) containing ~40 year old trees of the Northern Hardwood forest association (Hales et al., 2009). The Hollow Trench was excavated by a backhoe to 2 m depth revealing a colluvial soil composed of three major horizons, a 0.4 m A horizon, a 0.8 to 1.0 m B horizon, containing angular

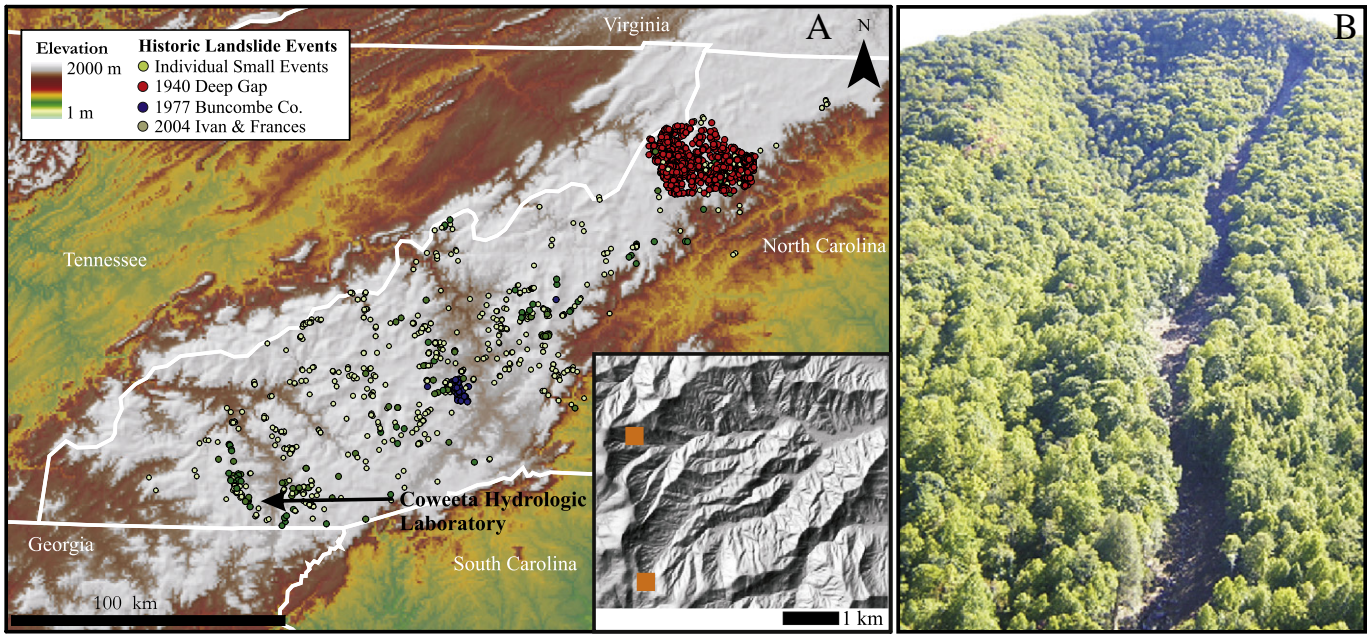

Fig. 1. Southern Appalachian Mountains. (A) Digital elevation model of the North Carolina Appalachian Mountains with points showing the locations of initiation zones of historic landslides mapped by the North Carolina Geological Survey (Witt, 2005). The NCGS mapping effort has concentrated on three North Carolinian counties (Macon, Watauga, and Buncombe). Historical events are dominated by extreme tropical storm precipitation, the largest events in 1940, 1977, and 2004 are highlighted. Inset shows location of field sites (orange squares) within Coweeta. (B) Photograph of the Peek's Creek debris flow track, North Carolina. The debris flow occurred in a soil mantled landscape, with distinctive ridges and hollows.

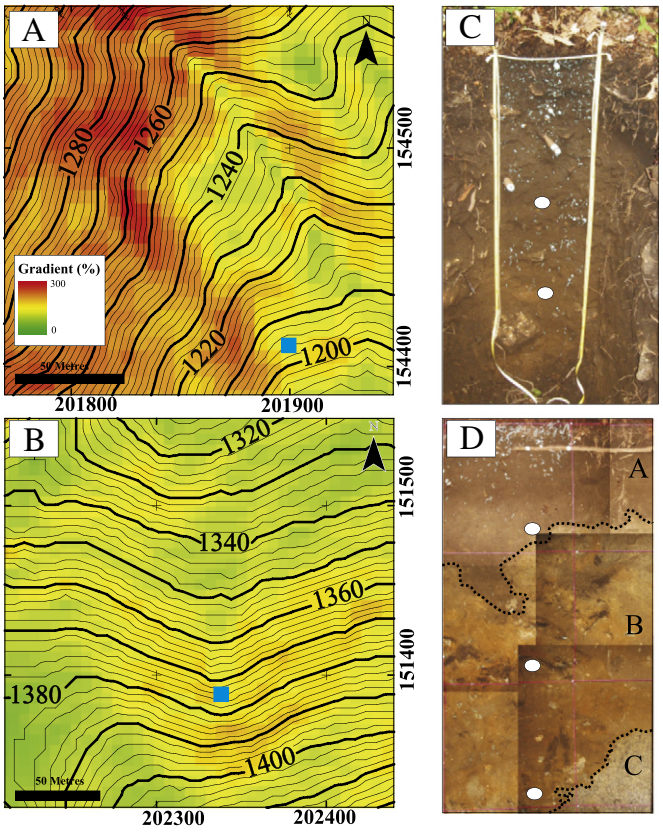

Fig. 2. Map and photograph of each hollow analysed in this study. Gradient and contour map (2 m contour interval) of (A) Pit 13 (located by the blue square) and (B) Hollow Trench. Photographs of the pit walls showing the sample locations (white circles) in (C) Pit 13 and the (D) Hollow Trench. The irregular soil boundaries in the Hollow Trench that distinguish the A, B, and C horizons are shown by the dotted lines. Maps are both in UTM coordinate system.

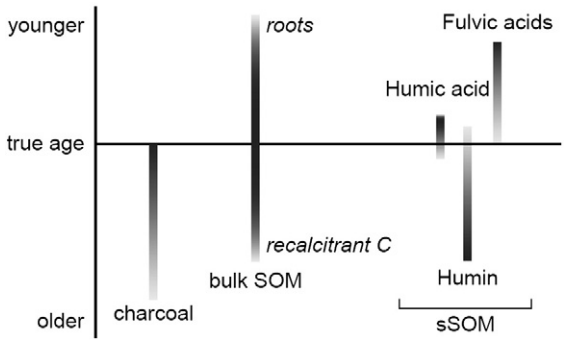

Fig. 3. Plot of radiocarbon age of physical and chemical fractions of soil relative to true age of deposit. Absent bioturbation, charcoal provides a maximum age. Varying quantities of roots or recalcitrant charcoal can cause wide range of age of bulk SOM. sSOM is typically dominated by recalcitrant C and thus eliminates most contamination from roots, here we show range of different chemical fractions of the sSOM. In this study we dated charcoal and both humic acid and humin portions of the sSOM.

cobbles of saprolitic material, and an irregular C horizon (Fig. 2D). In this location, there is no significant accumulation of cobbles or boulders at the base of the hollow, suggesting that there has been no significant accumulation of periglacial material since the last evacuation event. One litre bags of soil were extracted using a trowel at 0.4 and 0.9 m, and also at the soil–saprolite contact at 1.4 m. Pit 13 (Fig. 2B) is located at a lower elevation in a long, narrow hollow ~300 m downslope from the rim of the Nantahala Mountains Escarpment, in Watershed 36. The pit was excavated by hand to 1.8 m depth, close to the stability limit of our pit walls. At this site the A horizon transitioned to an AB horizon at a depth of ~80 cm, but the soil–saprolite contact was not reached. We sampled soil and charcoal at depths of 0.7 and 1.4 m.

2.2. Radiocarbon analysis

Obtaining a "true" age of a soil is challenging because soils consist of a mix of carbon sources that accumulate and degrade by complex chemical and biological processes (Marschner et al., 2008). In order to capture effect of these processes on the estimated age of a soil, it is common practice to isolate and date different physical and chemical fractions of the soil (Fig. 3; Trumbore and Zheng, 1996; Bird et al., 2002). One of the most common physical separations is to date individual pieces of charcoal (>1 mg) from the soil (Reneau et al., 1989; Pessenda et al., 2001). In principle, charcoal should provide a maximum age of soil formation due to the delay between burning of the plant and burial in the soil. Documentation of stratigraphic consistency of charcoal dates (i.e. deeper samples are older) is commonly used to argue that transport times and bioturbation were minimal (e.g. Scharer et al., 2007). Other physical separations avoid problems due to episodic delivery of charcoal (limited by local fire frequency) and date the soil more directly. One of the most common physical separations is simply bulk soil organic material (SOM). SOM provide minimum ages because juvenile radiocarbon is continually added at the surface from leaf litter and other surficial carbon sources, and then mixed into the soil column by ecologic and geomorphic activity. Unfortunately, contamination with young roots and biological activity can result in SOM ages that are so much younger than the soil (Wang et al., 1996; Pessenda et al., 2001). A third physical separation is the isolation of the silt fraction of the SOM (sSOM). A significant body of work in the past decade has shown that carbon in the sSOM, especially pyrogenic C and lignin, has a long residence time and thus can provide another estimate of the maximum age (Gleixner et al., 2001; Ponomarenko and Anderson, 2001; Skjemstad et al., 2002; Heim and Schmidt, 2007; Marschner, 2008). Pyrogenic C includes a wide spectrum of material from condensed aromatic black carbon to partially burnt plant material and is fairly resistant to biochemical degradation. Lignin is the second most abundant constituent of wood, and should be prevalent in Appalachian soils because the slopes have been forested throughout the late Quaternary (Delcourt, 1979). However, while lignin production is continuous (unlike pyrogenic C, which is limited by fire frequency), lignin is more prone to degradation than pyrogenic C and may not be preserved over long periods in the sSOM (Marschner et al., 2008). In summary, lignin and pyrogenic C contribute to sSOM ages that are usually maximum ages of the soil; if pyrogenic C is prevalent, the sSOM can be significantly older than the age of the soil itself whereas if lignin provides a greater contribution, the resultant date will provide a better estimate of the time since the soil was at the surface.

Chemical fractions of organic material are used to further isolate or eliminate different humic substances from soils, principally fulvic acid, humic acid, and humin, based on their solubility (Trumbore, 2000; Wershaw, 2000; Scharer et al., 2007). Fulvic acids are soluble in most pH conditions and are normally removed in radiocarbon samples because they can include atmospheric sources of young carbon. Humic acids are base soluble and thought to result from the degradation of lignin and other organic substances (Stevenson, 1982; Shevchenko and Bailey, 1996). Humin is not soluble under natural pH conditions and is possibly an early product of the soil forming process. Humin is isolated by removal of humic acid and fulvic acid thought a series of acid and base chemical pretreatments; in effect lignin and other resistant organic materials such as fine pyrogenic C and pollen remain the humin fraction.

Due to these complications, we dated paired sSOM and charcoal samples to explore the contributions of various carbon sources, to provide improved understanding of the age of hollow evacuation and refilling, and to track transport of older material into the hollow from the side slopes. Physical separation into the sSOM followed procedures outlined in similar studies (e.g. Trumbore and Zheng, 1996; Bird et al., 2002). Approximately 500 cm^3 of each sample was soaked in deionized water to disaggregate and then wet sieved through #10, #60 and #230 sieves. The fine fraction (<63 μm) was dried in a covered Pyrex dish (either in an oven or on a hot plate, neither exceeded 60 °C), and submitted to the Lawrence Livermore National Laboratory for chemical pretreatment. Isolation of the humin fraction of the sSOM was achieved by standard acid–alkali–acid pretreatment (1 N HCl, 1 N NaOH) before combustion. We also collected the base soluble portion of the sSOM in order to date the humic acid fraction of both deep (140 cm) samples. Individual charcoal fragments (>2 mg) were collected from the coarse fractions of the soils and chemically pretreated following standard acid–alkali–acid pretreatment.

2.3. Calculating hillslope erosion rates

Our data can be used to estimate the volumetric infilling rate in each hollow. These data can, in turn, be used to estimate bedrock erosion rates for slopes contributing material to the hollow. If we assume that all of the material deposited in a hollow is derived from soil produced and transported within the catchment upslope of the hollow, it is possible to create a conservation of mass expression for the hillslope-averaged bedrock erosion rate in a catchment (E):

$$\frac{\rho_b}{\rho_s}E = I + \Delta S + V_{out} \tag{1}$$

where I is the volumetric infilling rate of soil in the hollow, ΔS is any change in the volume of soil stored in the hillslopes (i.e. a change in average soil thickness through time), V_{out} is any soil material removed from the hollow by landsliding or soil creep, and ρ_b and ρ_s are bedrock and soil densities respectively. We measure the infilling rate by dating horizons in each hollow. ΔS cannot be measured, so we assume that there has been no significant change in average soil thickness over the Holocene. The lack of evidence for a periglacial contribution to hollow sedimentation, the low elevation of our sites relative to periglacial deposits in the Great Smoky Mountains (Nelson et al., 2007), and the early- to mid-Holocene age of our basal dates suggest that a forested landscape has existed in the catchments studied during the infilling of the hollows. Therefore, the most parsimonious assumption is that there has been no significant change in soil thickness with time. Thus Eq. (1) can be rewritten:

$$E = \frac{1}{A}\frac{\rho_s}{\rho_b}\left(\frac{dV_h}{dt} + \frac{dV_{out}}{dt}\right) \tag{2}$$

where A is the contributing drainage area, t is the radiocarbon-derived time interval over which soil was deposited, and V_h is the volume of soil in a hollow between two dated horizons (Reneau et al., 1989). Estimating volume of material deposited in a hollow requires knowledge of the bedrock geometry of the hollow, which is difficult to measure. Our samples were collected on a vertical pit face, in which it is possible to estimate the width and depth of the deposit. This allows the problem to be reduced to two dimensions, where the change in cross sectional area of the pit per unit time reflects the erosion rate of the length of hillslope that contributes directly to the sample locations minus any material that is removed. In the two-dimensional case, the gradient of the hollow is considered constant immediately upslope and downslope of the excavated pit face. As the erosion rate attributable to creep is dependent on slope (Davis, 1892; Gilbert, 1909; McKean et al., 1993) no change in gradient means that any material eroded down the axis of the hollow is replaced by material immediately upslope (a more detailed derivation of this method can be found in Reneau et al., 1989). This means that there is no net loss (or gain) of soil from the hollow axis and accumulation of material in the hollow is solely due to input from the two side slopes immediately adjacent to the hollow axis (l_1 and l_2, respectively),

$$E = \frac{\sum_{z_{n-1}}^{z_n}\int w_z dz}{dt}\frac{\rho_s}{\rho_b(l_1 + l_2)} \tag{3}$$

where z_n is the depth of each dated horizon, and w_z is the depth integrated width (Fig. 4).

We report maximum and minimum erosion rates for each of our dated horizons using Eq. (3). Maximum erosion rates were estimated by assuming the youngest possible age for the deposit, with minimum rates derived from the oldest possible ages. The most significant sources of uncertainty in our data are associated with the different dating methods (as noted in Section 2.2) and our estimates of the width and depth of the hollow. We assessed the magnitude of uncertainty in hollow geometry and radiocarbon dating using a Monte Carlo simulation. In the simulation, deposit width, hillslope length, deposit thickness, soil and bedrock density, and radiocarbon age were randomly sampled from uniform distributions bounded by the maximum and minimum estimated values. Hillslope length and deposit width were estimated from a LiDAR derived digital elevation model flown for North Carolina with a grid spacing of 20 ft (~7 m) (http://www.ncfloodmaps.com; Fig. 2). Hillslope length was calculated as the maximum upslope flowpath length based on the D8 flow algorithm (using the Whitebox Geospatial Analysis Tools algorithm, http://www.uoguelph.ca/~hydrogeo/Whitebox/index.html). Hollow width was estimated as the transition between concave and planar topography as shown on a map of profile curvature. For both the length and width of the hollows the primary source of uncertainty is in the quality of the LiDAR data. For both length and width estimates we have assumed an uncertainty of one pixel (±7 m) for both the hillslope length and hollow width. We measured deposit thickness directly in the Hollow Trench, but estimated the thickness of Pit 13 as a minimum of 1.4 m and a maximum of 3.0 m, based on the maximum thickness of hollow soils observed in road cuts in the Coweeta Basin. Soil and bedrock densities were estimated as varying between 1600 and 1800 kg m^{-3} and 2600–3000 kg m^{-3} (Turcotte and Schubert, 2002). A relatively constant production of charcoal and pyrogenic C is assumed based on the prevalence of Holocene charcoal in the southern Appalachians (Fesenmeyer and Christensen, 2010). Without a priori knowledge of the charcoal production rate through time, we use the uniform distribution as the most parsimonious attempt to estimate dating errors. We ran the Monte Carlo simulation 10,000 times to encapsulate the full range of uncertainties in all parameters and have reported the uncertainty as a standard deviation in calculated erosion rates.

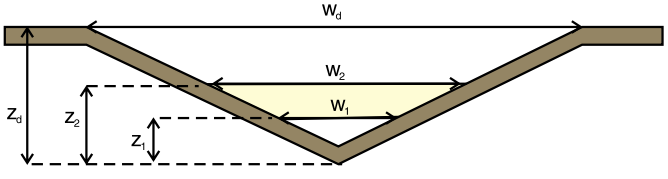

Fig. 4. Schematic diagram of hollow showing the parameters used to calculate hollow volume. The yellow box shows the area between two dated horizons (w_1 and w_2) at depths z_1 and z_2. Erosion rate is calculated using Eq. (3).
Modified from Reneau et al. (1989).

3. Results

3.1. Radiocarbon dates

We dated three horizons in the Hollow Trench and two in Pit 13 (Fig. 5, Table 1). At each site, the charcoal dates considered alone are stratigraphically consistent, and the sSOM dates, with one exception, are equal or older than the charcoal date at any given horizon. Overall stratigraphic consistency suggests that significant mixing of the soil column (i.e. below the active soil depth at any time) did not occur over the course of hollow refilling. We have paired charcoal and sSOM dates from four horizons. Of these, one of the most significant results is the ages obtained from 140 cm in Pit 13 (P140), in which the charcoal piece and both humic acid and humin fractions of the sSOM produced a similar age (~6000 year BP). Because humic acids are produced from the degradation of lignin and other substances, they are typically younger than the humin fraction of the soil (Rethemeyer et al., 2005). Given the range of organic sources in these samples, similarity of the P140 dates suggests that ~6000 (+/−230) years provides a good estimate of the time since this horizon was at the ground surface. The P140 dates also show that the sSOM date from 70 cm in Pit 13, which is ~2000 years older but 70 cm higher, likely contained a significant fraction of recalcitrant carbon and provides a measure of the amount of variability (1000s of years) of available carbon sources from any given horizon. Since the charcoal ages are stratigraphically consistent and thus bioturbation is limited to the active soil horizon (~top 30 cm), we infer that recalcitrant pyrogenic C also contributed to the sSOM age 40 cm in the Hollow Trench (H40), which is 5000 years older than a charcoal date from the same horizon. Unfortunately, the sSOM from 140 cm (H140) was loamy sand that contained no utilisable humic acids, so we have no date for this fraction in the Hollow Trench.

3.2. Hillslope erosion rates

We calculated erosion rates for each dated horizon; a maximum erosion rate using the youngest age of each horizon and where available, a minimum using the oldest age at each horizon (Table 2). Variation in calculated rates is less for Pit 13 than the Hollow Trench, largely due to the young piece of charcoal at 40 cm in the Hollow Trench. Overall erosion rates show a consistent pattern through time; starting low at ~0.01 mm yr^{-1} between basal and intermediate horizons, and then increasing during the filling of the upper half of the hollows (since about 2 to 3 ka) to 0.03 to 0.4 mm yr^{-1}.

In Pit 13, basal ages determined from three different types of carbon varied between 5733 and 6272 years old and put a tight constraint on the potential age of material. When the total variability in these ages is included in the Monte Carlo simulation, we calculate an average erosion rate of 0.042 ± 0.003 mm yr^{-1} at that interval. Uncertainty in these erosion rates is primarily derived from the assumed geometry of the hollow, in particular, the hollow width and depth. This uncertainty has a non-linear effect on the estimate of erosion rates and justifies the use of the Monte Carlo approach. The minimum rate from 70 cm in Pit 13 (0.031 ± 0.002 mm yr^{-1}) is based on a sSOM date that is stratigraphically inconsistent with dates below.

A wider distribution of dates exists for the Hollow Trench and requires a careful interpretation of the erosion rates. At 140 cm two ~24 ka pieces of charcoal are considerably older than any other material found within either hollow. The Hollow Trench is located just below a relatively flat region above the Nantahala escarpment (Fig. 2), so we suggest that long residence time on the plateau or incomplete evacuation of the hollow during the previous landsliding event explains why the basal charcoal samples are significantly older than the sSOM and stratigraphically higher charcoal samples. Possibilities for increasing the residence time include incomplete evacuation of material during previous landsliding events, or headward erosion of the basin into plateau sediments that contain older charcoal. Incomplete hollow evacuation was observed in the Peek's Creek landslide that evacuated during the storms of 2004 (Wooten et al., 2008). The total headward erosion of the basin over 20,000 years of erosion is less than 50 cm, so incorporation of very old charcoal derived from this plateau seems unlikely. Due to these concerns about the genesis of the charcoal, the younger sSOM age is our best estimate of the last evacuation of the Hollow Trench (Fig. 3). The mean erosion rate calculated using the humin-fraction of the sSOM at 1.40 m suggests that the hillslopes around the Hollow Trench erode at ~0.1 mm yr^{-1}. Humin-derived rates from 0.40 m in the Hollow Trench are similar (0.122 mm yr^{-1}). These rates are bracketed by the range of charcoal-derived dates (0.008–0.824 mm yr^{-1}), highlighting the possible episodic delivery of soil and colluvium to the hollow.

With a wide range of erosion rate estimates for different combinations of horizons, the challenge is how to interpret these data. For the maximum erosion rate estimates, calculated using the minimum ages, the range of calculated ages varies between 0.008 and 0.824 mm yr^{-1}. The range is not an accurate representation of the results as it highlights the anomalously high and low erosion rates. We consider the central tendency and variability of the rate estimates as a better way to represent these results. For the maximum calculated

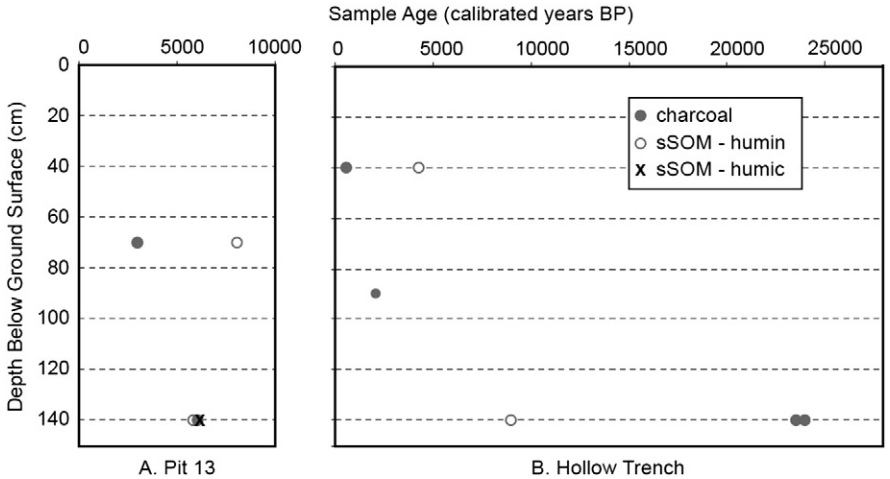

Fig. 5. Stratigraphic plot of radiocarbon results. Calibrated uncertainties are smaller than diameter of symbols. The charcoal ages are stratigraphically consistent, and with one exception, equal to or younger than the sSOM ages.

Table 1
Radiocarbon ages and hollow geometries for each of our samples.

Site name	Sample ID	Lab ID	Deposit width (w_d) (m)	Contributing basin width (m)	Distance below western ridge (m)	Distance below eastern ridge (m)	Depth of ^{14}C (m)	Uncalibrated ^{14}C age (years)	Error (years)	Calibrated ^{14}C age (years)	Error (years)
Hollow Trench	H-40-m	137313	30	70	85	73	0.4	3835	30	4278	129
Hollow Trench	H-40-c	137314	30	70	85	73	0.4	525	30	569	61
Hollow Trench	H-90-c1 *	135623	30	70	85	73	0.9	2100	30	2071	76
Hollow Trench	H-140-m-aaa *	135618	30	70	85	73	1.4	8080	30	8960	162
Hollow Trench	H-140c2 *	135621	30	70	85	73	1.4	23,990	120	23,989	238
Hollow Trench	H-140-c3	135622	30	70	85	73	1.4	23,540	130	23,546	265
Pit 13	13-70-c	135624	14	56	103	201	0.7	2840	40	2964	112
Pit 13	13-70-m	137315	14	56	103	201	0.7	7230	35	8065	95
Pit 13	13-140-m-hu*	135730	14	56	103	201	1.4	5350	35	6137	136
Pit 13	13-140-m-aaa *	135619	14	56	103	201	1.4	5055	30	5818	85
Pit 13	13-140-c	135620	14	56	103	201	1.4	5270	40	6058	123

erosion rates from both hollows the mean is 0.171 mm yr^{-1} (with a standard error of 0.091 mm yr^{-1}) and the median is 0.046 mm yr^{-1}. We argue that the charcoal at 40 cm depth in the Hollow Trench is unreliable as it is at a depth that is prone to bioturbation and produces anomalous results (both the minimum and maximum rates are calculated using that age). The mean erosion rate calculated when you exclude those calculations that use the anomalous age changes to 0.111 mm yr^{-1} (with a standard error of 0.060 mm yr^{-1}) and the median is 0.069 mm yr^{-1}. The average minimum erosion rate is 0.051 mm yr^{-1} (with a standard error of 0.025 mm yr^{-1}). Alternately, it is possible to consider the most reliable ages as those estimated across the longest time span, from the basal age to the present (Pit 13 at 0.042 ± 0.003 mm yr^{-1} and the Hollow Trench at 0.106 ± 0.006 mm yr^{-1}). The inclusion of the single age at 40 cm in the Hollow Trench affects the data considerably, whereas its removal produces a mean erosion rate that is consistent with erosion rates measured at the longest timescales. These mean erosion rates are derived from multiple independent estimates and we suggest they are more reliable than quoting any single erosion rate. As a result, we consider the average maximum erosion rate, excluding the erroneous value at 40 cm in the Hollow Trench as the most reliable estimate. Thus we quote the 0.111 and 0.051 mm yr^{-1} erosion rates as the most robust estimates of the maximum and minimum erosion rates.

4. Discussion

4.1. Dating colluvial soils

Organic material in soil accumulates and degrades by complex pathways related to particle size, soil chemistry, and unknown contributions of both "old" and "young" carbon. Because residence times (or turnover rates) for each organic compound can vary (Glaser, 2005; Heim and Schmidt, 2007), no single method exists to determine the age of a progressively buried soil and the best approach is to date a wide variety of materials such that the range of possible ages brackets this complex process (Fig. 3). In this study, we compared sSOM and charcoal ages to determine the timing of soil formation as the hollows progressively infilled. The humin fraction of the sSOM typically represents maximum ages because it tends to accumulate recalcitrant carbon, especially pyrogenic C attached to silt and clay (Trumbore and Zheng, 1996; Marschner et al., 2008).

Although we have dated only two sites, our results have implications for the utility of radiocarbon for studies of hillslope erosion. First, overall stratigraphic consistency suggests that these Appalachian hollows fill progressively, a pattern not always seen in accumulating soil sequences (e.g. Carcaillet, 2001; Gavin, 2003). Second, there is a large reservoir of stable carbon in southern Appalachian forest soils. Charcoal is particularly common, and as shown in other studies (e.g., Fesenmeyer and Christensen, 2010), 4000 year old and even earliest Holocene charcoal can be found in modern soils. These observations underscore the availability of recalcitrant carbon in active soil horizons. Recalcitrant carbon available in the active soil horizon may contribute to sSOM dates that are older than the associated charcoal (at P70 and H40) and the Pleistocene charcoal samples at H140. In total, by examining different fractions of the buried soils and the availability of charcoal in the system, we ascertain that the oldest age at any horizon provides a robust maximum age of the soil at that level, and convergence of the humic acid, humin sSOM and charcoal age of P140 suggests that the youngest charcoal ages provide a good minimum estimate for these accumulation rates.

Table 2
Estimates of hillslope erosion rates (in mm yr^{-1}) for our two hollows.

Horizon	Average maximum rate	Standard deviation (max. rate)	Average minimum rate	Standard deviation (min. rate)
Hollow Trench				
0–40	0.824	0.068	0.122	0.007
0–90	0.401	0.023	–	–
0–140	0.106	0.006	0.047	0.003
40–90	0.046	0.003	–	–
40–140	0.008	0.000	0.004	0.001
90–140	0.010	0.001	–	–
Pit 13				
0–70	0.096	0.005	0.031	0.002
0–140	0.042	0.003	–	–
70–140	0.011	0.001	–	–

4.2. Hillslope erosion rates in the Appalachian context

There is a large amount of erosion rate information available for the Appalachian Mountains, at a range of spatial (individual hillslopes to orogen-averaged scales) and temporal (10^1 to 10^7 years) scales. Accounting for the caveats associated with over-interpreting small datasets, we will attempt to put our hillslope creep erosion rates in the wider context of orogenic erosion. Erosion rates calculated at individual sites have focused on the understanding processes of fluvial incision, periglacial erosion, shallow landsliding, and mechanical weathering of bedrock. Our data are collected in hollows and reflect erosion of short, shallow hillslopes, primarily by creep processes. These rates contrast periglacial erosion rates of between 0.1 and 0.3 mm yr^{-1}, estimated from volume of scree and talus slopes or debris fan deposits (Hack, 1965; Braun, 1989; Eaton et al., 2003a). Fluvial incision rates in Appalachian river systems are an order of magnitude lower than periglacial rates and 1.5–4 times lower than hillslope erosion rates at ~0.03 mm yr^{-1} (Granger et al., 2001). Bedrock weathering rates estimated using cosmogenic radionuclide dating of flat upland bedrock surfaces are an order of magnitude lower again at 0.002–

0.0095 mm yr^{-1} (Granger et al., 2001; Hancock and Kirwan, 2007). When put in the context of these other data, our average minimum and maximum erosion rate estimates fall between the periglacially-derived bedrock erosion rates and fluvial incision rates (Hack, 1965; Braun, 1989; Granger et al., 2001). This suggests that the processes driving hillslope erosion are decoupled from the fluvial boundary condition, an observation that is supported by the evidence for large alluvial plains separating hillslopes from the larger channels. In areas of steeper relief, such as in the Coweeta Hydrologic Laboratory channels incise into bedrock, suggesting that hillslope erosion in these areas is soil production limited. This is something that could be tested in greater detail with a larger dataset. Rate comparisons between periglacial and hillslope erosion suggest that scree and talus slope production is slightly more efficient than the creep processes that infill the Coweeta hollows.

Hillslope erosion rates are up to two orders of magnitude higher than catchment-scale erosion rates estimated in the Southern Appalachians. Sediment yields for the major catchments that drain the Southern Appalachians suggest short-term (<50 years) denudation rates of 0.006 to 0.039 mm yr^{-1} (Judson and Ritter, 1964; Hack, 1979; Conrad and Saunderson, 1999). Much of the sediment contributing to these rates (up to 63%) is derived from debris flows initiated in hollows (Eaton et al., 2003b). Cosmogenically-derived catchment erosion rates of 0.025 to 0.030 mm yr^{-1} from the Great Smoky Mountains (Matmon et al. 2003a,b) are similar to the short-term rates. Our minimum average erosion rates are similar to the maximum catchment erosion rates; however, the central tendency of these datasets is different enough to suggest a disconnect between hillslope sediment production and the processes controlling catchment sediment yield.

4.3. Comparison with estimates of hillslope creep

Quantifying rates of specific erosional processes at geomorphic timescales is challenging, as is reflected the relatively small number of process rates found within the literature. Our calculations use the unique geometry of hollows, which contain material that can only be derived directly from the hillslopes above. For relatively short hillslopes, such as those used in this study, creep erosion dominates. For forested landscapes, creep erosion is thought to be driven by tree throw and, potentially, burrowing animals (Roering et al., 2002; Hales et al., 2009). It follows that hillslope creep erosion rates from forested landscapes should be controlled by the distribution of root biomass and its penetration into rock (Roering et al., 2010). Complicated relationships exist between root biomass and climate, ecology, soils, and geology within different geographical regions (Jackson et al., 1996) that could possibly create large discrepancies between erosion rates measured in different regions. However, this variability is not as significant as the difference between the deeply penetrating root systems of trees and shallow grassland roots (Roering et al., 2002). The hillslope erosion rates presented here, collected in a temperate deciduous forest, can be readily compared with data collected using the same methods in the temperate coniferous forests of the Pacific Northwest (Fig. 6). Southern Appalachian hillslope erosion rates of between 0.051 and 0.111 mm yr^{-1} are consistent with the rates derived from these forest ecosystems, despite dramatically different geology, climate, and ecology (Dietrich and Dorn, 1984; Reneau et al., 1989; Reneau and Dietrich, 1990, 1991). Fig. 6A shows the distribution of hillslope erosion rates measured for the three mountain ranges where hillslope erosion is estimated by dating hollow fill (Reneau et al., 1989; Reneau and Dietrich, 1990). There is a consistent median erosion rate of ~0.1 mm yr^{-1} for each of the three mountain ranges, suggesting that tree throw and other mechanisms driving hillslope erosion in forested landscapes may operate at relatively consistent rates across a wide range of environmental conditions. Consistent hillslope erosion rates for the Western U.S. and the southern Appalachian mountains, despite the wide range of environmental conditions, suggest that erosion is dominated by tree-related processes rather than the ecology or geology of an area.

These similar hillslope erosion rates occur within landscapes that have a difference in long-term spatially-averaged erosion rates of two orders of magnitude (Pazzaglia and Brandon, 2001; Matmon et al., 2003a). This suggests that while hillslopes are eroding at the same rate in each landscape, hillslope erosion is of reduced importance in the overall sediment budget of the Appalachians when compared to the Oregon Coast Range and the Olympic Mountains. Such contributions are reflected in the topography of each mountain range; long-term erosion rates correlate with the distribution of hillslope area (Fig. 6B). The Olympic Mountains contain long hillslopes that contribute sediment directly to steep rivers as is shown by the distribution of slopes within the mountain range, which have a median of 21%. A greater proportion of steep slopes suggests that the hillslopes are more closely connected to the fluvial system and there is a greater number of hillslopes contributing sediment to the fluvial system. Long-term erosion rates in this mountain range are considerably higher than the creep rates suggesting that landsliding and other non-linear processes may contribute significantly to the sediment budget (Montgomery and Brandon, 2002). The slope distribution for the Oregon Coast Range is significantly different from that of the Olympic Mountains. The Oregon Coast Range has a median slope of 10% and a right-skewed slope distribution (Fig. 6B). Hillslopes in this landscape tend to be shorter than the Olympic Mountains, with rivers carving relatively broad floodplains. Erosion rates measured at many spatial scales in this landscape (Heimsath et al., 2001) are consistent with hillslope erosion rates measured in hollows (Reneau et al., 1989; Reneau and Dietrich, 1991). This suggests that hillslope creep is an important and possibly dominant erosional process in this mountain range. The southern Appalachians have the lowest median slope (6%) and long-term erosion rates are much lower than hillslope erosion rates. The southern Appalachian have hillslopes that are concentrated in escarpment-like mountains separated by wide river

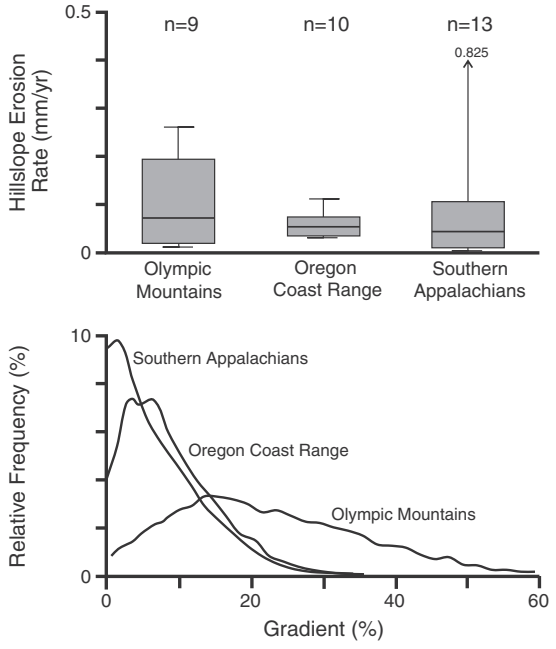

Fig. 6. Comparison of hillslope erosion rates for forested mountains in the United States. (A) Comparison of erosion rates determined by similar approach as whisker and box plots (Reneau et al., 1986, 1989; Reneau and Dietrich, 1990). The boxes represent the interquartile range of erosion rate estimates with the bold line in the centre representing the median erosion rate. The lines represent the 95% and 5% values. (B) The frequency distribution of slope angles within the southern Appalachians, Oregon Coast Range, and Olympic Mountains derived from 30 arc sec GTOPO30 digital elevation models.

valleys, and hillslope sediment liberated from hollows has long residence times on floodplains (Leigh and Webb, 2006). Thus the relatively small area of Appalachian hillslope means that spatially-averaged erosion rates are lower than those for other mountains.

5. Conclusions

We present estimates of hillslope erosion rates for steep, colluvial hollows in the Southern Appalachian Mountains, North Carolina. We determined the stratigraphic distribution of sediment age within each hollow by radiocarbon dating pieces of charcoal and the silt fraction of soil organic material. Both fractions can be equal to or older than the soil age, but in combination can be used to understand the transport history of material into the hollow. We use these different estimates to bracket the soil age and accommodate uncertainty in dating progressively filled hollows. We calculate hillslope erosion rates by estimating the accumulation of soil contributed from the side slopes between each stratigraphic horizon. Hillslope erosion rate estimates of for the two hollows are 0.051 and 0.111 mm yr^{-1} since ~8 ka and represent the first hillslope creep rates estimated for the Appalachian Mountains. These rates are consistent with other estimates of hillslope erosion in forested mountains with faster long-term erosion rates. Our results suggest that long term erosion in the Southern Appalachians is governed by the transfer of sediment from the relatively small, steep hillslopes to the sedimentary system, and that this process is fairly efficient.

Acknowledgements

We would like to thank Jim Vose and Larry Band for supporting the field component of this research, and Richard Whittecar, Takashi Oguchi, and an anonymous reviewer for their constructive comments. Daniel Band and Jenny Riker provided extensive help with shovel and paint brush. Thanks also to Tom Guilderson at Lawrence Livermore National Laboratory for providing radiocarbon analyses. Appalachian State University students Aaron Pruitt and Chesney Gilleland prepared our radiocarbon samples.

References

Bird, M., Santuckova, H., Lloyd, J., Lawson, E., 2002. The isotopic composition of soil organic carbon on a north–south transect in Western Canada. Eur. J. Soil Sci. 53, 393–403.
Braun, D.D., 1989. Glacial and periglacial erosion of the Appalachians. Geomorphology 2, 233–256.
Carcaillet, C., 2001. Soil particles reworking evidences by AMS ^{14}C dating of charcoal. Earth Planetary Sci. 332, 21–28.
Carson, M.A., Kirkby, M.J., 1972. Hillslope Form and Process. Cambridge University Press, Cambridge. 475 pp.
Clark, G.M., 1987. Debris slide and debris flow historical events in the Appalachians south of the glacial border. Rev. Eng. Geol. 7, 125–138.
Clark, G.M., Ciolkosz, E.J., 1988. Periglacial geomorphology of the Appalachian Highlands and Interior Highlands south of the glacial border—a review. Geomorphology 1, 191–220.
Conrad, C.T., Saunderson, H.C., 1999. Temporal and spatial variation in suspended sediment yields from eastern North America. In: Smith, B.J., Whalley, W.B., Warke, P.A. (Eds.), Uplift, Erosion and Stability. Geological Society, London, Special Publications. Geological Society, London, pp. 219–228.
Davis, W.M., 1892. The convex profile of bad-land divides. Science 20, 245.
Delcourt, H.R., 1979. Late Quaternary vegetation history of the eastern Highland Rim and adjacent Cumberland Plateau of Tennessee. Ecol. Monogr. 49, 255–280.
Delcourt, H.R., Delcourt, P.A., Webb III, T., 1982. Dynamic plant ecology: the spectrum of vegetational change in space and time. Quat. Sci. Rev. 1, 153–176.
Dietrich, W.E., Dorn, R., 1984. Significance of thick deposits of colluvium on hillslopes — a case study involving the use of pollen analysis in the Coastal Mountains of Northern California. J. Geol. 92, 147–158.
Dietrich, W.E., Dunne, T., 1978. Sediment budget for a small catchment in mountainous terrain. Z. Geomorphol. Suppl. 29, 191–206.
Eaton, L.S., Morgan, B.A., Craig, K.R., Howard, A.D., 2003a. Quaternary deposits and landscape evolution of the central Blue Ridge of Virginia. Geomorphology 56, 139–154.
Eaton, L.S., Morgan, B.A., Kochel, R.C., Howard, A.D., 2003b. Role of debris flows in long-term landscape denudation in the central Appalachians of Virginia. Geology 31, 339–342.
Fesenmeyer, K.A., Christensen, N.L., 2010. Reconstructing Holocene fire history in a southern Appalachian forest using soil charcoal. Ecology 91, 662–670.
Field, C.B., Behrenfeld, M.J., Randerson, J.T., Falkowski, P., 1998. Primary production of the biosphere: integrating terrestrial and oceanic components. Science 281, 237–240.
Gabet, E.J., Reichman, O.J., Seabloom, E., 2003. The effects of bioturbation on soil processes and hillslope evolution. Ann. Rev. Earth Planetary Sci. 31, 249–273.
Gavin, D., 2003. Forest soil disturbance intervals inferred from soil charcoal radiocarbon dates. Can. J. For. Res. 33, 2514–2518.
Gilbert, G.K., 1909. The convexity of hillslopes. J. Geol. 17, 344–350.
Glaser, B., 2005. Compound-specific stable-isotope ($\delta^{13}C$) analysis in soil science. J. Plant Nutr. Soil Sci. 168, 633–648.
Gleixner, G., Czimczik, C., Kramer, C., Luhker, B., Schmidt, M., 2001. Plant compounds and their turnover and stabilization as soil organic matter. In: Schulze, E.-D., Heimann, M., Harrison, S., Holland, E., Lloyd, J., Prentice, I.C., Schimel, D. (Eds.), Global Biogeochemical Cycles in the Climate System. Academic Press, San Diego, pp. 201–206.
Granger, D.E., Fabel, D., Palmer, A.N., 2001. Pliocene–Pleistocene incision of the Green River, Kentucky, determined from radioactive decay of cosmogenic ^{26}Al and ^{10}Be in Mammoth Cave sediments. Geol. Soc. Am. Bull. 113, 825–836.
Hack, J.T., 1965. Geomorphology of the Shenandoah Valley Virginia and West Virginia and the origin of residual ore deposits. USGS Professional Paper 484, 84 p.
Hack, J.T., 1979. Rock control and tectonism—their importance in shaping the Appalachian highlands. USGS Professional Paper 1126-B, 17 p.
Hack, J.T. Goodlett, J.C., 1960. Geomorphology and forest ecology of a mountain region in the central Appalachians. USGS Professional Paper 347, 66 p.
Hales, T.C., Ford, C.R., Hwang, T., Vose, J.N., Band, L.E., 2009. Topographic and ecologic controls on root reinforcement. J. Geophys. Res. 114. doi:10.1029/2008JF001168.
Hancock, G., Kirwan, M., 2007. Summit erosion rates deduced from ^{10}Be: implications for relief production in the central Appalachians. Geology 35, 89–92.
Heim, A., Schmidt, M., 2007. Lignin is preserved in the fine silt fraction of an arable Luvisol. Org. Geochem. 38, 2001–2011.
Heimsath, A.M., Dietrich, W.E., Nishiizumi, K., Finkel, R.C., 2001. Stochastic processes of soil production and transport: erosion rates, topographic variation and cosmogenic nuclides in the Oregon Coast Range. Earth Surf. Processes Landf. 26, 531–552.
Hursh, C.R., 1941. The geomorphic aspects of mudflows as a type of accelerated erosion in the Southern Appalachians. Am. Geophys. Union Trans. 2, 253–254.
Hwang, T., Band, L.E., Hales, T.C., 2009. Ecosystem processes at the watershed scale: extending optimality theory from plot to catchment. Water Resour. Res. 45. doi:10.1029/2009WR007775.
Jackson, R.B., Canadell, J., Ehleringer, J.R., Mooney, H.A., Sala, O.E., Schulze, E.D., 1996. A global analysis of root distributions for terrestrial biomes. Oecologia 108, 389–411.
Judson, S., Ritter, D.F., 1964. Rates of regional denudation in the United States. J. Geophys. Res. 69, 3395.
Leigh, D.S., Webb, P.A., 2006. Holocene erosion, sedimentation, and stratigraphy at Raven Fork, Southern Blue Ridge Mountains, USA. Geomorphology 78, 161–177.
Marschner, B., Brodowski, S., Dreves, A., Gleixner, G., Gude, A., Grootes, P.M., Hamer, U., Heim, A., Jandl, G., Ji, R., Kaiser, K., Kalbitz, K., Kramer, C., Leinweber, P., Rethemeyer, J., Schaffer, A., Schmidt, M., Schwark, L., Wiesenberg, G.L.B., 2008. How relevant is recalcitrance for the stabilization of organic matter in soils? J. Soil Sci. Plant Nutr. 171, 91–110.
Marschner, B.A.O., 2008. How relevant is recalcitrance for the stabilization of organic matter in soils? J. Soil Sci. Plant Nutr. 171, 91–110.
Matmon, A., Bierman, P.R., Larsen, J., Southworth, S., Pavich, M.J., Caffee, M., 2003a. Temporally and spatially uniform rates of erosion in the southern Appalachian Great Smoky Mountains. Geology 31, 155–158.
Matmon, A., Bierman, P.R., Larsen, J., Southworth, S., Pavich, M.J., Finkel, R.C., Caffee, M., 2003b. Erosion of an ancient mountain range, the great Smoky Mountains, North Carolina and Tennessee. Am. J. Sci. 303, 817–855.
Matsuoka, N., 1998. The relationship between frost heave and downslope soil movement: field measurements in the Japanese Alps. Permafr. Periglac. Process. 9, 121–133.
McKean, J.A., Dietrich, W.E., Finkel, R.C., Southon, J.R., Caffee, M., 1993. Quantification of soil production and downslope creep rates from cosmogenic ^{10}Be accumulations on a hillslope profile. Geology 21, 343–346.
Mills, H.H., 1982. Long-term episodic deposition on mountain foot slopes in the Blue Ridge Province of North Carolina; evidence from relative-age dating. Southeast. Geol. 23, 123–128.
Mills, H.H., 1983. Pediment evolution at Roan Mountain, North Carolina, USA. Geogr. Ann. 65A, 111–126.
Mills, H.H., Allison, J.B., 1995. Controls on variation of fan-surface age in the Blue Ridge Mountains of Haywood County, North Carolina. Phys. Geogr. 15, 465–480.
Montgomery, D.R., Brandon, M.T., 2002. Topographic controls on erosion rates in tectonically active mountain ranges. Earth Planetary Sci. Lett. 201, 481–489.
Nelson, K.J.P., Nelson, F.E., Walegur, M.T., 2007. Periglacial Appalachia: paleoclimatic significance of blockfield elevation gradients, eastern USA. Permafr. Periglac. Process. 18, 61–73.
Pazzaglia, F.J., Brandon, M.T., 2001. A fluvial record of long-term steady-state uplift and erosion across the Cascadia forearc high, western Washington State. Am. J. Sci. 301, 385–431.
Pessenda, L.C.R., Gouveia, S.E.M., Aravena, R., 2001. Radiocarbon dating of total soil organic matter and humin fraction and its comparison with ^{14}C ages of fossil charcoal. Radiocarbon 43, 595–601.
Ponomarenko, E., Anderson, D., 2001. Importance of charred organic matter in Black Chernozem soils of Saskatchewan. Can. J. Soil Sci. 18, 285–297.

Reneau, S.L., Dietrich, W.E., 1990. Depositional history of hollows on steep hillslopes, Coastal Oregon and Washington. Natl. Geogr. Res. 6, 220–230.
Reneau, S.L., Dietrich, W.E., 1991. Erosion rates in the Southern Oregon Coast Range: evidence for an equilibrium between hillslope erosion and sediment yield. Earth Surf. Processes Landf. 16, 307–322.
Reneau, S.L., Dietrich, W.E., Dorn, R.I., Berger, C.R., Rubin, M., 1986. Geomorphic and paleoclimatic implications of latest Pleistocene radiocarbon dates from colluvium-mantled hollows, California. Geology 14, 655–658.
Reneau, S.L., Dietrich, W.E., Rubin, D.M., Donahue, D.J., Jull, A.J.T., 1989. Analysis of hillslope erosion rates using dated colluvial deposits. J. Geol. 97, 45–63.
Rethemeyer, J., Kramer, C., Gleixner, G., John, B., Yamashita, T., Flessa, H., Andersen, N., Nadeau, M.-J., Grootes, P.M., 2005. Transformation of organic matter in agricultural soils: radiocarbon concentration versus soil depth. Geoderma 128, 94–105.
Roering, J.J., Almond, P.C., Tonkin, P., McKean, J., 2002. Soil transport driven by biological processes over millenial time scales. Geology 30, 1115–1118.
Roering, J.J., Marshall, J., Booth, A.M., Mort, M., Jin, Q., 2010. Evidence for biotic controls on topography and soil production. Earth Planetary Sci. Lett. 298, 183–190.
Scharer, K.M., Weldon, R.J., Fumal, T.E., Biasi, G.P., 2007. Paleoearthquakes on the southern San Andreas fault, Wrightwood, CA 3000 to 1500 B.C.: a new method for evaluating paleoseismic evidence and earthquake horizons. Bull. Seismol. Soc. Am. 97, 1054–1093.
Schumm, S.A., 1967. Rates of surficial rock creep on hillslopes in Western Colorado. Science 15, 560–562.
Shevchenko, S.M., Bailey, G.W., 1996. Life after death: lignin–humic relationships reexamined. Crit. Rev. Environ. Sci. Technol. 26, 95–154.
Skjemstad, J.O., Reicosky, D.C., Wilts, A.R., McGowan, J.A., 2002. Charcoal carbon in U.S. agricultural soils. Soil Sci. Soc. Am. J. 66, 1249–1255.
Stevenson, F.J., 1982. Humus Chemistry — Genesis, Chemistry, Reactions. John Wiley and Sons, New York. 443 pp.
Swift, L.W., Cunningham, G.B., Douglass, J.E., 1988. Climatology and hydrology. In: Swank, W.T., Crossley, D.A. (Eds.), Forest Hydrology and Ecology. Springer, New York, pp. 35–55.
Taylor, S.B., Kite, J.S., 2006. Comparitive geomorphic analysis of surficial deposits at three central Appalachian watersheds: implications for controls on sediment-transport efficiency. Geomorphology 78, 22–43.
Trumbore, S., 2000. Radiocarbon geochronology. In: Noller, J.S., Sowers, J.M., Lettis, W. (Eds.), American Geophysical Union Reference Shelf 4, pp. 41–60.
Trumbore, S.E., Zheng, S.H., 1996. Comparison of fractionation methods for soil organic matter C-14 analysis. Radiocarbon 38, 219–229.
Turcotte, D.L., Schubert, G., 2002. Geodynamics. Cambridge University Press, Cambridge. 456 pp.
Wang, Y., Amundson, R., Trumbore, S., 1996. Radiocarbon dating of soil organic matter. Quat. Res. 45, 282–288.
Wershaw, R.L., 2000. The study of humic substances — in search of a paradigm. In: Ghabbour, E.A., Davies, G. (Eds.), Humic Substances, Versatile Components of Plants, Soils, and Water. The Royal Society of Chemistry, Cambridge, pp. 1–7.
Wieczorek, G.F., Mossa, G.S., Morgan, B.A., 2004. Regional debris-flow distribution and preliminary risk assessment from severe storm events in the Appalachian Blue Ridge Province, USA. Landslides 1, 53–59.
Witt, A.C., 2005. A brief history of debris flow occurrence in the French Broad River watershed, western North Carolina. N. C. Geogr. 13, 58–82.
Wooten, R.M., Latham, R.S., Witt, A.C., Fuemmeler, S.J., Gillon, K.A., Douglas, T.J., Bauer, J.B., 2006. Slope Movement Hazard Maps of Macon County, North Carolina, N.C. Geological Survey Geologic Hazards Map Series 1, Raleigh, North Carolina.
Wooten, R.M., Latham, R.S., Witt, A.C., Gillon, K.A., Douglas, T.J., Fuemmeler, S.J., Bauer, J.B., Reid, J.C., 2007. Landslide hazards and landslide hazard mapping in North Carolina. In: Schaefer, V.R., Schuster, R.L., Turner, A.K. (Eds.), 1st North American Landslide Conference. Association of Environmental and Engineering Geologists, Vail, Colorado, pp. 458–471.
Wooten, R.M., Gillon, K.A., Witt, A.C., Latham, R.S., Douglas, T.J., Bauer, J.B., Fuemmeler, S.J., Lee, L.G., 2008. Geologic, geomorphic, and meteorological aspects of debris flows triggered by Hurricanes Frances and Ivan during September 2004 in the Southern Appalachian Mountains of Macon County, North Carolina (southeastern USA). Landslides 5, 31–44.
Wooten, R.M., Witt, A.C., Gillon, K.A., Douglas, T.J., Fuemmeler, S.J., Bauer, J.B., Latham, R.S., 2009. Slope Movement Hazard Maps of Buncombe County, North Carolina, N.C. Geological Survey Geologic Hazards Map Series 4, Raleigh, North Carolina.
Yoo, K., Amundson, R., Heimsath, A., Dietrich, W.E., 2005. Process-based model linking pocket gopher (*Thomomys bottae*) activity to sediment transport and soil thickness. Geology 33, 917–920.